infrastructures

MDPI

Article

Fatigue Reliability Assessment of Bridges Under Heavy Traffic Loading Scenario

Mingyang Zhang [1], Xuejing Wang [2] and Yaohan Li [2,*]

[1] College of Civil and Transportation Engineering, Shenzhen University, Shenzhen 518060, China; zhang601@szu.edu.cn
[2] Department of Construction and Quality Management, Hong Kong Metropolitan University, Hong Kong SAR, China; xuwang@hkmu.edu.hk
* Correspondence: yahli@hkmu.edu.hk

Abstract: Uncertainties in traffic flows pose significant challenges for the accurate fatigue safety assessment of bridge structures. Fatigue analysis requires detailed information on heavy vehicle-induced loads, which can be obtained from weigh-in-motion (WIM) systems. This paper develops a stochastic traffic load model based on site-specific WIM measurements to evaluate the fatigue reliability of steel bridges by enhancing simulation efficiency and incorporating correlations in traffic load parameters. Traffic loading is measured on site by WIM systems and used to develop a probabilistic model. A heavy traffic scenario load model is developed based on the Gaussian mixture model (GMM) and Poisson distribution. The correlation between traffic load parameters is addressed using the Nataf transformation. The fatigue reliability of critical components is evaluated using this procedure as an illustrative example. The results show that annual increases in traffic load significantly impact fatigue damage. This research provides a theoretical basis for improved traffic management and structural maintenance strategies.

Keywords: fatigue; reliability; traffic load; weigh in motion; traffic growth

Citation: Zhang, M.; Wang, X.; Li, Y. Fatigue Reliability Assessment of Bridges Under Heavy Traffic Loading Scenario. *Infrastructures* **2024**, *9*, 238. https://doi.org/10.3390/infrastructures9120238

Academic Editor: Boulent Imam

Received: 6 November 2024
Revised: 12 December 2024
Accepted: 18 December 2024
Published: 20 December 2024

1. Introduction

Fatigue is one of the most critical forms of deterioration in steel bridges, and the accumulation of fatigue damage is a major cause of collapse in these structures [1–5]. For instance, a large-span steel box girder suspension bridge, constructed in 1997 in southern China, demonstrates the importance of addressing fatigue-related issues. The primary deterioration observed within the steel box girder comprised fatigue cracks in the transverse diaphragms, the U-ribs, and the joints with the top plate. In 2008, visually detectable fatigue cracks were identified within the steel box girder for the first time, with a total of 129 occurrences across the bridge. From 2009 onwards, the number of fatigue cracks has increased by varying extents each year. As of the scheduled inspection in May 2017, a total of 929 fatigue cracks had been identified throughout the bridge [6]. Steel bridges are repeatedly subjected to variable-amplitude vehicle loads, resulting in the gradual accumulation of fatigue damage [7]. This poses serious threats to the structural safety of key components, accelerates material deterioration, and shortens the service life of bridges. The eventual fracture resulting from accumulated fatigue damage is a significant concern in bridge health management [4,5]. Therefore, it is essential to assess the fatigue performance and predict the service life of steel bridges under operational conditions.

Traffic load plays a crucial role in determining the service performance and fatigue deterioration behavior of bridges. Fatigue damage in bridges caused by vehicle loads is directly influenced by stress amplitude and the frequency of load cycles. In fatigue-resistant design and safety assessment, it is common to use either standardized fatigue load models or models based on measured load data. Design codes such as BS 5400, AASHTO, Eurocode, and D64 develop corresponding fatigue load models based on each

country's traffic characteristics [8–11]. However, due to regional differences in economic conditions, production patterns, and traffic loads, the fatigue load models used in design may not accurately represent the actual loads experienced by bridges in service. Meanwhile, increasing traffic volume and gross vehicle weight (GVW) have posed a threat to the fatigue safety of existing bridges [12–18].

With advancements in structural health monitoring (SHM) technology, reliable data on traffic load and structural responses can be collected [5,19]. Meanwhile, probabilistic updating of structural models using Bayesian inference has been extensively studied in the field of SHM [20]. This shift presents a new paradigm for assessing and predicting structural performance, with monitoring data being used to reduce epistemic uncertainties associated with deterioration processes. This leads to more precise assessments of structural performance and predictions of service life. Numerous studies have focused on utilizing monitoring data to predict the remaining fatigue life of bridges. Frangopol et al. [21] proposed a method that integrates SHM data into structural reliability assessments to enhance predictive accuracy and optimize maintenance strategies. Kwon and Frangopol [22] proposed an approach for the fatigue reliability assessment and prediction of steel bridges by using probability density functions (PDFs) based on field monitoring data. Ni et al. [23] developed a fatigue reliability model that combines hot-spot stress distribution with Miner's damage rule, using long-term strain data from the Tsing Ma Bridge to evaluate fatigue life and reliability. Di et al. [24] arranged strain gauges at the hot-spot stress extrapolation position of the welded parts to obtain strain–time history data. The fatigue performance of the orthotropic steel bridge decks was assessed using two weeks of monitoring data on hot-spot stress. These studies have shown the potential of SHM-based data for enhancing fatigue life predictions. However, real-time measurements are costly and site-specific.

The numerous critical points where bridge structures are vulnerable to fatigue substantially increase the cost and complexity of implementing health monitoring systems. Additionally, current monitoring data cannot predict structural fatigue behavior as traffic flow characteristics evolve. Therefore, advanced research is needed to simulate fatigue responses based on modeled traffic flow data. With the aid of weigh-in-motion (WIM) technology, key vehicle characteristics, including type, speed, wheelbase, and axle weight, can be efficiently collected [25–27]. These data allow for the development of stochastic traffic models used for bridge condition assessment [28]. Guo et al. [29] utilized WIM data from the Throgs Neck Bridge (USA) to characterize the probability distributions of axle weights, spacings, and vehicle positions. By combining WIM data with stochastic traffic flow simulation, researchers have proposed traffic modeling methods to evaluate the extreme responses induced by vehicle loads [30–32]. Such simulations have proven effective in modeling extreme traffic scenarios and estimating future maximum load effects. The use of WIM data helps to evaluate the effects of traffic loads on bridge safety and structural integrity. Wang et al. [33] utilized WIM data to establish probability models for vehicle parameters, simulating traffic flow through agent-based microsimulation. Structural responses were then obtained by integrating the traffic flow model with finite element (FE) analysis. Gao et al. [34] proposed a novel simulation method of the compound Poisson process based on the stochastic harmonic function to represent the stochastic traffic load process so that the fatigue damage of concrete bridges under traffic loading can be efficiently and accurately evaluated. Meanwhile, numerous recent studies have emerged to address the corrosion–fatigue-coupled deterioration of steel bridges. Fan et al. [35] developed a reliability analysis framework for the suspenders of a long-span suspension bridge, incorporating on-site WIM data and corrosion fatigue analysis. This approach accounted for time-varying corrosion effects and long-term traffic growth. Zhu et al. [36] presented the probabilistic deterioration of corrosion fatigue in welded joints of weathering steel bridges, particularly focusing on rib-to-deck joints, which are considered fracture-critical. They proposed a three-stage probabilistic model to track crack growth under uncertainty. Based on traffic measurements, in [37], a stochastic traffic model was developed in a sampling-based

manner. In this model, a total of 100,000 vehicles are simulated to derive the fatigue stress spectra, capturing the variability in traffic loadings that influence the deterioration process.

The cellular automaton (CA) method has gained attention for simulating traffic flow on bridges due to its precision in modeling random traffic loads at a microscopic level [38,39]. This approach has been foundational in creating a framework for capturing the variability of stochastic traffic loads, especially for long-span bridges [40]. Notably, Ruan et al. [38] incorporated axis information into the CA model, enhancing its capability for the detailed microsimulation of random traffic loads on long-span bridges. This refined CA model offers an analytical basis that accurately reflects the complex and variable patterns of traffic flow. However, the CA model does not account for the correlation between traffic load parameters, such as vehicle weight, axle load, and speed. This omission limits the accuracy of fatigue damage predictions, as vehicle interactions play a significant role in determining the loads on the bridge structure. Additionally, the CA method can be inefficient when simulating the performance of existing bridges, particularly for long-span bridges where complex vehicle interactions are common [38]. While the CA method provides valuable insights into the microscopic dynamics of traffic flow, its limitations highlight the need for more comprehensive models that integrate traffic load parameter correlations and site-specific characteristics.

Recent advancements have highlighted the advantages of site-specific bridge loading models, which can result in significant cost savings during rehabilitation. These models provide a more accurate representation of actual loading conditions, avoiding the biases associated with code-based load models. Meanwhile, traffic growth presents considerable complexity due to the substantial variability and unpredictability of traffic data. Consequently, accounting for traffic growth is crucial in the evaluation of fatigue reliability. To overcome the deficiencies of the current research on the microscopic dynamics of traffic flow simulation in fatigue reliability assessment, this study aims to develop a stochastic traffic load model based on site-specific WIM data to assess the fatigue reliability of steel bridges. Additionally, a fatigue life prediction method is proposed by applying a heavy traffic scenario model to bridge influence lines, thereby improving the efficiency of fatigue life assessments. In addition, this study evaluates the impact of traffic growth on fatigue reliability assessment and provides insights for optimizing lifecycle management and structural maintenance strategies.

2. Methodology for Fatigue Reliability Assessment of Steel Bridge

To ensure the long-term performance and safety of steel bridges under traffic loads, it is critical to perform a fatigue reliability assessment that accounts for the stochastic nature of traffic flow and the accumulation of fatigue damage over time. Additionally, the correlation between truck weights in freight traffic can also influence the accumulation of fatigue damage. A two-stage probabilistic method is proposed for assessing the fatigue reliability of steel bridges under stochastic traffic loading. The fatigue reliability assessment integrates the statistical analysis of traffic loads with fatigue life prediction based on stress influence lines. The methodology is illustrated in Figure 1. The goal of the first stage is to establish basic models of traffic loads accounting for the correlation between heavy vehicles, while the second stage focuses on determining reliability.

In the first stage, real-world traffic data collected via WIM systems are statistically processed to establish a stochastic traffic flow model. The WIM system captures critical vehicle parameters, including GVW, axle loads, speeds, the number of axles, etc. [41]. The data collection process utilized real-time monitoring to capture vehicle parameters as vehicles passed over the WIM devices. These devices measure the axle loads with high precision. Over a one-year period, the system recorded more than 36 million vehicle transits on a 52 km segment of the A3 highway in southern Italy, creating an extensive dataset representative of actual traffic conditions. Comprehensive data filtering and quality assurance processes were applied to ensure the reliability of the dataset, including the removal of spurious or duplicate entries and the validation of vehicle dimensions and

weights. The dataset was further processed to derive the PDFs of key traffic parameters, such as GVW and vehicle positions on the bridge deck. These distributions serve as the foundational input for generating realistic stochastic traffic load models for bridge fatigue analysis. Further details on the WIM dataset and its processing are presented in Section 3.1. The correlation between the traffic load parameters is considered by employing the Nataf transformation method. The actual stress history is generated by applying the simulated traffic flow on the stress influence line.

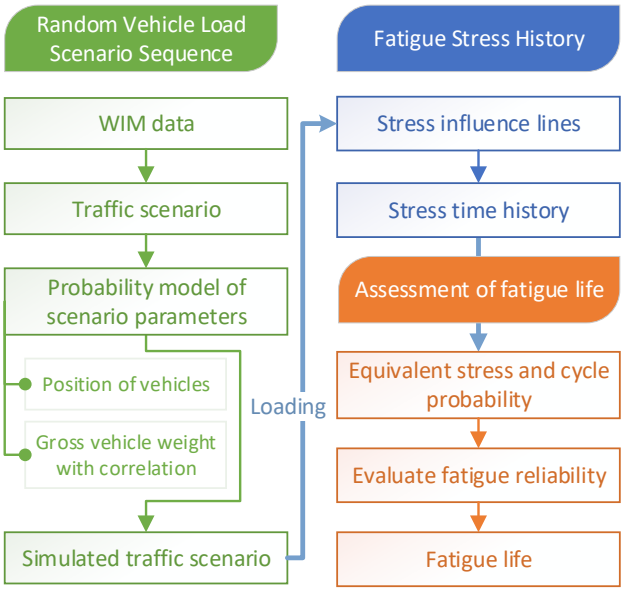

Figure 1. Framework of the fatigue life assessment method.

In the second stage, the bridge fatigue reliability is assessed using Monte Carlo simulations. The stress history obtained from the influence line is used to calculate cumulative fatigue damage based on the Palmgren–Miner linear damage rule. Reliability is then evaluated by considering the associated demand and capacity. In the following sections, the methodology for the fatigue reliability assessment of steel bridges and the procedure for stochastic traffic modeling will be introduced.

3. Heavy Traffic Load Sequence Model

3.1. Description of the WIM Database

The WIM data collected in Italy served as the foundation for the traffic load model. The data were collected from a WIM system installed on the A3 Napoli–Pompei–Salerno highway in southern Italy [41]. The A3 is a major transportation infrastructure that connects two key cities in the Campania region and provides direct links to the ports of Naples and Salerno in the Mediterranean Sea. This highway also serves the Sorrento and Amalfi coasts. The WIM data, covering the period from 6 August 2022 to 6 September 2022, comprise millions of vehicle records (3,039,725). Each record provides key information, including (1) the date and time of measurement; (2) the vehicle's total weight, length, and width; (3) vehicle speed and acceleration; (4) the axle numbers; (5) each axles' load, width, and distance from other axles of the same vehicle; and (6) the left/right partitioning of each axle's load. While the dataset is site-specific, it offers a realistic representation of highway traffic flow in terms of vehicle types and load distributions. The characteristics of this dataset, particularly the traffic mix and the presence of heavy vehicles, are common to many highways in Europe and other developed regions. Therefore, the results from this dataset can be considered applicable to similar road networks with comparable traffic conditions. More details about the WIM data can be found in [41]. It also should be noted that dataset may not fully represent traffic characteristics in all global contexts, especially

in regions with significantly different traffic patterns. Its generalization to other regions may require careful consideration of local traffic patterns.

Figure 2 shows that the daily traffic volume based on one month of WIM data fluctuates around 100,000 vehicles, with heavy vehicle flow (vehicles over 2 tons) fluctuating around 40,000 vehicles per day. The threshold of 2 tons is selected due to the fact that lighter vehicles induce stress amplitudes below the fatigue limit, insufficient to cause cumulative fatigue damage within the bridge structure's designed stress range [42]. Figure 3 shows the segmented distribution of gross vehicle weight. The selected WIM data indicate that vehicle weights are primarily concentrated in the range of 3 tons for lightweight vehicles. Additionally, there are noticeable peaks around 18 tons and 45 tons, displaying a characteristic multi-peak distribution pattern.

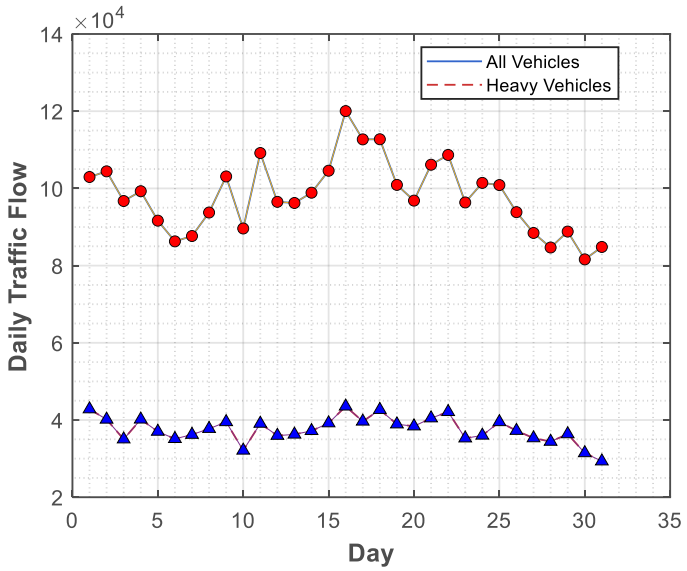

Figure 2. Daily traffic flow trends for all vehicles and heavy vehicles.

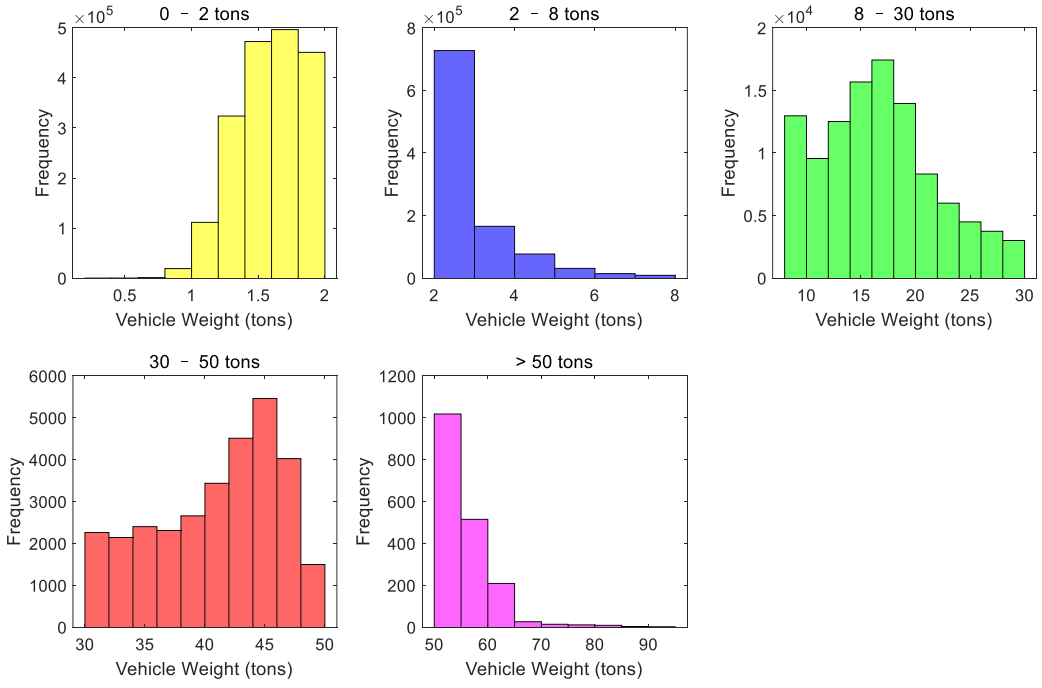

Figure 3. Segmented distribution of GVW in WIM data.

3.2. Probabilistic Model of Vehicle Load Parameters

From observation, it can be seen that the vehicle weight distribution exhibits distinct multimodal characteristics that cannot be accurately described by typical unimodal probability distribution models. To better represent these multimodal attributes, the Gaussian mixture model (GMM) is employed, as it effectively captures the presence of multiple peaks in the data. This finding is also consistent with previous studies on traffic flow [27,43,44]. Thus, the vehicle weight was modeled using a GMM. For the vehicle weight, χ, the PDF of the GMM can be expressed as Equation (1):

$$p(\chi) = \sum_{k=1}^{K} \pi_k N(\chi|\mu_k, \Sigma_k) \tag{1}$$

where $N(\chi|\mu_k, \Sigma_k)$ is the PDF of the k-th Gaussian distribution with μ_k and Σ_k as its mean and covariance matrix, and the parameter π_k denotes the weight of the k-th Gaussian distribution component, satisfying $\sum_{k=1}^{K} \pi_k = 1$ and $0 \leq \pi_k \leq 1$.

It is widely recognized that GVWs are correlated within the same lane and between adjacent lanes. Nowak [45,46] investigated the correlations of GVWs for trucks in the same and adjacent lanes, identifying three levels of correlation—no correlation, partial correlation, and full correlation—with corresponding Pearson correlation coefficients of 0, 0.5, and 1.0, respectively. Simulations revealed that full GVW correlation significantly impacts two-lane traffic loading, a finding validated through site observations. Similarly, O'Brien and Enright [47] found correlations between successive trucks' GVWs using WIM data from the EU, with inter-lane correlations influenced by lane spacing. Zhou et al. [48] further observed a 5% autocorrelation for trucks within a 5 s time gap. In this paper, it is assumed that a correlation exists between the weights of heavy vehicles in adjacent sections. The correlation length in the autocorrelation function for GVWs is estimated in the proposed traffic model. To simulate this correlation, the Nataf transformation method is applied. This method effectively establishes a connection between the standard Gaussian space and the original probability space, allowing for the generation of correlated random samples in the original space based on independent standard Gaussian samples. The whole procedure of a Nataf transformation involves two steps. The first step is to transform the independent standard normal variables G into the correlated standard normal variables Z with a correlation coefficient matrix R_z. The second step converts the correlated standard normal variables into variables denoted by χ (i.e., vehicle weight following GMM distribution). This transformation is depicted in [49].

$$\begin{cases} Step1: Z \rightarrow U = L \cdot G \\ Step2: U \rightarrow \chi_i = F_{\chi_i}^{-1}[\Phi(U)] \end{cases} \tag{2}$$

where L satisfies the equation $R_z = LL^{\mathrm{T}}$, in which L is a lower triangular matrix and can be obtained by means of Cholesky decomposition on R_z. $\Phi(\cdot)$ is the cumulative distribution function of a standard normal variable. $F_{\chi_i}^{-1}[]$ is the inverse of the cumulative distribution function of the variable χ_i, which follows the GMM distribution. R_z needs to be determined first according to the correlation coefficient matrix R_χ at the beginning of the Nataf transformation. In this process, the R_χ of GVWs is calculated by the exponential autocorrelation function.

3.3. Vehicle Position Modeling

In the context of heavy traffic scenarios, an appropriate probability distribution must be determined to model the occupancy of cells by heavy vehicles on specific lanes. Using a statistical analysis of the number of cells occupied by heavy vehicles in each lane, the single-lane spatial distribution for heavy vehicles is modeled by a Poisson process. It is assumed that the number of cells occupied by heavy vehicles within the loading length L follows a Poisson process. The probability of t occupied cells can be determined as follows:

$$P(T_L = t) = \frac{(\lambda L)^t exp(-\lambda L)}{t!}, \quad t = 0,\ 1,\ 2, \ldots \tag{3}$$

where $P(\cdot)$ represents the probability of the event, and λ denotes the average rate of vehicle occupancy in the cells. For a stationary distribution process of heavy vehicles, λ remains constant across the entire loading length.

3.4. Simulation of Heavy Traffic Scenario

The simulation process for representation is as follows: (1) The bridge deck is divided into 1 m cells within each lane. (2) Based on WIM data, heavy traffic (vehicles over 2 tons) scenario samples are obtained, where the scenario length corresponds to the bridge length, with a total of 500 heavy vehicle scenario samples collected from the WIM data. (3) The parameters of the heavy vehicle weight distribution and the Poisson process parameters for heavy vehicle positions within the sample scenarios are calculated. Figure 4 compares the simulation results of the number of heavy vehicles per lane with the WIM sample. Figure 5 presents the weight distribution histogram of heavy vehicles in the sample scenarios along with a GMM fitting. During fitting, the number of GMM sub-distributions is set to six, as illustrated by the Akaike information criterion (AIC) plot in Figure 6, which confirms that selecting six components is reasonable. (4) For each lane, a heavy vehicle weight is assigned to the cell by employing a GMM and Nataf transformation. With the Nataf transformation, a sequence of vehicles with specific correlations between pairs of heavy vehicles can be simulated over a defined correlation length (100 m was selected in this study based on [34]), and this sequence satisfies the original GMM distribution. (5) Based on the Poisson process and heavy vehicle distribution characteristic parameters shown in Figure 4, a simulation of whether each cell in the lane is occupied by a heavy vehicle is carried out. If a cell is occupied, a heavy vehicle weight is assigned based on the values from step 4; if unoccupied, the weight is set to 0, as depicted in Figure 7. Note that, in this step, the number of heavy vehicles per lane in the simulated scenario is assigned based on the distribution parameters from Figure 4, followed by a Poisson distribution to simulate cells within the lane that contain heavy vehicles. (6) These steps are repeated for each lane to generate a set of heavy traffic sequences. Additionally, the average traffic speed determines the length of the monthly traffic sequence, simulating a monthly traffic flow sequence for subsequent loading on the stress influence line.

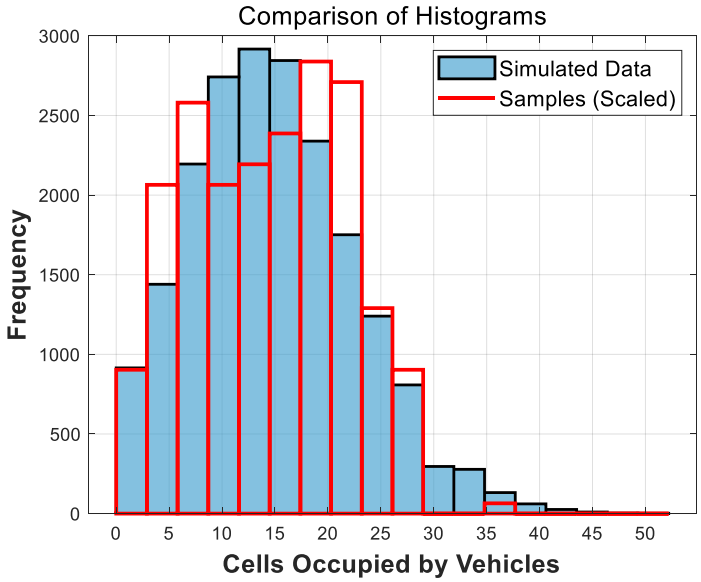

Figure 4. Comparison of the number of heavy vehicles per lane in simulated traffic scenarios and WIM data traffic scenarios.

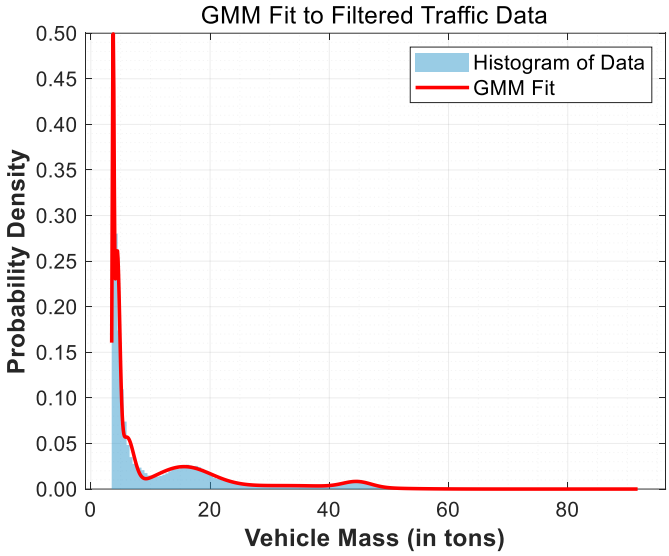

Figure 5. Distribution of heavy vehicle weights in traffic scenarios and GMM fitting.

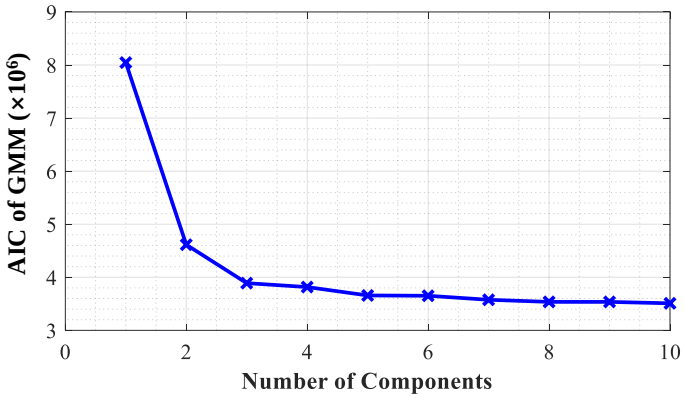

Figure 6. AIC curve for determining optimal number of components in GMM for heavy vehicle weight distribution.

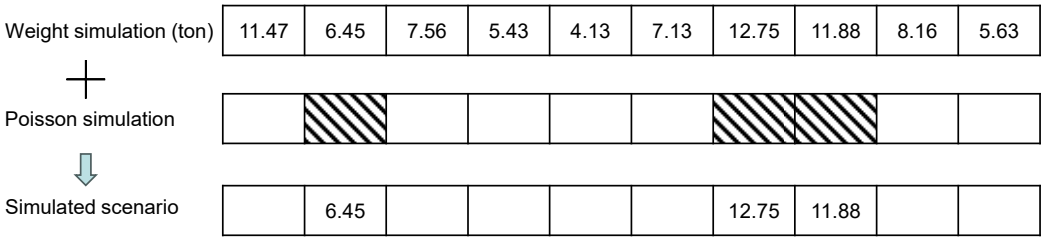

Figure 7. Schematic diagram of the traffic scenario simulation process.

4. Fatigue Stress–Time History

The accurate estimation of bridge fatigue life under stochastic traffic flow requires a reliable record of the fatigue stress–time history, which can be achieved by applying a simulated stochastic traffic load sequence to the bridge's stress influence line. Figure 8 illustrates the calculation of the response time history: as each vehicle crosses the bridge, it generates a corresponding set of response–time histories. The duration of each vehicle being on the bridge is determined by the bridge length divided by the vehicle speed, and the shape of these response–time histories corresponds to the shape of the influence line. Using three moving vehicles from the traffic flow as an example, Figure 8 demonstrates the loading principle behind stochastic traffic flow on influence lines with different vehicle speeds. In this study, vehicles are assumed to travel at a constant speed as they cross the bridge. It should be noted that this assumption simplifies the calculation of stress influence.

This assumption might not accurately represent the real-world variability in vehicle speeds, particularly in congested traffic, which can affect fatigue loads and, subsequently, the fatigue life of bridge components. The effects of the vehicles' speed on fatigue reliability will be addressed in a future study. When vehicles successively cross the bridge, the interval between the entry times of consecutive vehicles is denoted as t, with vehicle speeds represented as v_1, v_2, and v_3. The overall response–time history of the bridge, generated by the vehicles, is the linear superposition of their individual response–time histories. This method effectively captures the dynamic interaction between vehicle loads and the bridge, providing a reliable basis for predicting the bridge's fatigue life under stochastic traffic conditions.

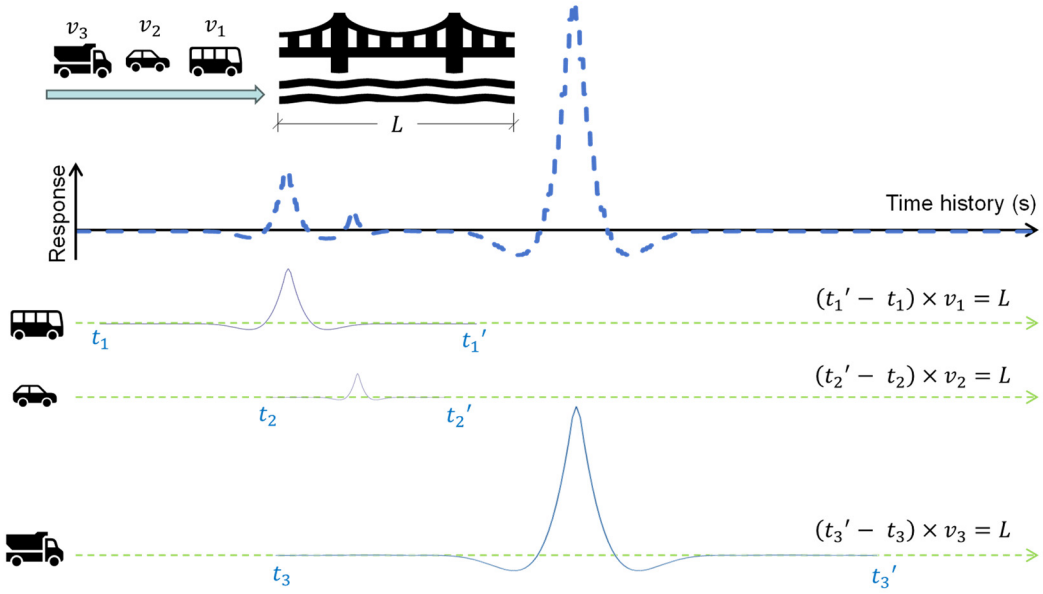

Figure 8. Calculation process of response–time history for target stress.

5. Fatigue Reliability Assessment

5.1. Fatigue Damage Analysis Under Heavy Traffic Scenario

Structural fatigue damage accumulates over the service life of bridges due to traffic loads. The fatigue failure of a structural component is typically assumed to occur when the cumulative fatigue damage reaches a critical threshold, corresponding to a certain number of stress cycles. The conventional approach for estimating structural fatigue damage accumulation combines the *S*-*N* curve with Miner's linear damage accumulation theory. While Miner's damage rule is widely used for estimating fatigue damage in structural components, it does have limitations when applied to stochastic traffic conditions, where the traffic loads exhibit significant variability. Specifically, Miner's rule assumes linear damage accumulation, and this assumption may not fully capture the complexities of real-world traffic. To address these limitations, future research could explore alternative models for fatigue damage that account for non-linear damage accumulation and sequence effects, such as Paris' law for crack growth. These models would allow for a more realistic representation of how fatigue damage develops under stochastic traffic conditions because the fatigue stress ranges induced by heavy traffic vary in amplitude due to the randomness of traffic loads. An equivalent stress range method based on the linear cumulative damage criterion provided in Eurocode 3 [50] was used in this study, expressed as follows:

$$D = \sum_{S_i \geq \Delta\sigma_D} \frac{n_i S_i^3}{K_C} + \sum_{S_i < \Delta\sigma_D} \frac{n_j S_j^5}{K_D} = \frac{N_{eq} S_{eq}^5}{K_D} \quad (4)$$

where D denotes the cumulative fatigue damage; $\Delta\sigma_D$ is the constant amplitude fatigue limit; S_i and S_j are the stress ranges; n_i is the number of stress range S_i (larger than $\Delta\sigma_D$)

and n_j refers to the number of stress range S_j (smaller than $\Delta\sigma_D$); and K_C and K_D represent the fatigue strength coefficients when $S_i \geq \Delta\sigma_D$ and $S_i < \Delta\sigma_D$, respectively, and are calculated as follows:

$$K_C = \Delta\sigma_C^3 \times 2 \times 10^6 \tag{5}$$

$$K_D = \Delta\sigma_D^5 \times 5 \times 10^6 \tag{6}$$

where $\Delta\sigma_C$ is the detail category. Based on the fatigue damage equivalence principle, the equivalent stress range and corresponding cycle count can be determined using the following equations:

$$S_{eq}^5 = \frac{\sum\limits_{S_i \geq \Delta\sigma_D} \frac{n_i S_i^3}{K_C} + \sum\limits_{S_i < \Delta\sigma_D} \frac{n_j S_j^5}{K_D}}{N_{eq}/K_D} \tag{7}$$

$$N_{eq} = \sum_{S_i \geq \Delta\sigma_D} n_i + \sum_{S_i < \Delta\sigma_D} n_j \tag{8}$$

In this study, the rainflow counting method is applied to the stress–time history generated by the simulated traffic load on the bridge. The rainflow counting algorithm extracts cycles from the stress history obtained from the simulation. As a result of the counting, several cycles and half-cycles with different amplitudes and mean values are obtained. This process involves rotating the stress–time history by 90° so that the time axis is oriented vertically downward, creating a visual representation of a pagoda roof. Hypothetical "rainflows" are then imagined to start at each extremum point (local maxima or minima) and descend along the "roof". A stress reversal, or half-cycle, is defined by tracking each rainflow as it continues downward until it either encounters a larger opposing extremum, intersects with another rainflow descending from a higher point, or drops below the level of the roof. Full cycles are subsequently formed by pairing reversals that meet these criteria, effectively delineating hysteresis loops. The rainflow counting method was implemented by using an algorithm in MATLAB 2023b [51].

5.2. Fatigue Reliability Analysis

Based on the limit-state function g(X) = *R*–*S*, the failure probability of a structural member can be defined as P_f = P(g(X) < 0). Given the stochastic nature of traffic flows, it is crucial to evaluate the uncertainty in structural fatigue damage and accurately predict the remaining fatigue life under repeated vehicle loading. Meanwhile, the vehicle load directly impacts fatigue life, and the life prediction model must account for traffic growth. This study assumes an annual increase in daily traffic volume, incorporating a growth coefficient to represent the increase in load cycles and simulate traffic flow growth. Using the fatigue stress history derived from influence line loading, the fatigue limit-state function (LSF) under stochastic traffic flow can be expressed as follows:

$$g(X) = D_f - D_f(t) = D_f - \frac{365 \times N_{eq} \times S_{eq}^5}{K_D}\left[1 + \sum_{i=1}^{t} \frac{veh_i}{veh_1}\right] \tag{9}$$

where D_f represents the critical fatigue damage of a bridge component; $D_f(t)$ is the accumulated damage at time t; and veh_1 and veh_i are the first and i-th year's annual daily truck traffic (ADTT), respectively.

The time-dependent fatigue reliability index for structural components can be defined using the following equation:

$$\beta = \Phi^{-1}\left(1 - P_f\right) = -\Phi^{-1}\left(P_f\right) \tag{10}$$

where P_f is the probability of failure and Φ^{-1} denotes the inverse standard normal cumulative distribution function (CDF).

6. Illustrative Examples

6.1. Stress Influence Line of the Key Component of Steel Bridges

A fatigue reliability analysis was conducted on a hypothetical four-lane steel bridge, with its stress influence line used as an illustrative example to demonstrate the effects of varying traffic loads on structural fatigue performance. The stress influence line considered in this study is illustrated in Figure 9. An exponential autocorrelation function was applied with an assumed 100 m correlation length to consider the associated traffic load parameter correlations. The selection of a 100 m correlation length was based on previous studies [31]. It should be noted that this length is a parameter within the model that could vary depending on the specific site conditions. The Monte Carlo method was utilized to assess the fatigue reliability. The Monte Carlo method generates a wide range of possible traffic scenarios by randomly sampling traffic parameters based on their probability distributions. By running multiple iterations, Monte Carlo simulations capture both typical and extreme traffic conditions, reflecting the full range of possible outcomes over the bridge's service life. This probabilistic approach enables the estimation of fatigue damage under varying traffic loads, improving the accuracy of fatigue life predictions. Furthermore, the simulations allow for the inclusion of rare but high-impact events, ensuring that extreme scenarios are considered in the reliability assessment. By employing a probabilistic model of the fatigue stress range, the fatigue reliability is evaluated over the bridge service life. In practice, traffic volume tends to increase alongside socioeconomic development. The growth of traffic volume cannot be ignored in the fatigue reliability assessment. In most studies, it is typically assumed to have a constant growth rate. However, such an assumption is oversimplified and lacks a solid basis. Therefore, this study considers growth in the ADTT by employing two models. These two models were developed based on data collected from a national database www.autostrade.it (accessed on 1 November 2024 covering the period from 1990 to 2020 [52]. The traffic volume growth models are presented in Table 1. The traffic volume is assumed to remain constant within every single year, with the variate average growth ratio serving as the growth coefficient of traffic volume between consecutive years. The effects of traffic growth on fatigue are studied by sampling stochastic traffic. Figure 10 represents the PDFs of response values obtained every second. The response distribution of the simulated traffic flow shows good agreement with the original WIM data. Moreover, the quality of the fitting results is quantified by the Kullback–Leibler divergence, D, defined in [53].

$$D(P \parallel Q) = \int_{-\infty}^{\infty} p(x) \ln\left(\frac{p(x)}{q(x)}\right) \tag{11}$$

where $p(x)$ and $q(x)$ denote the probability densities of the response obtained from WIM data and simulated data, respectively.

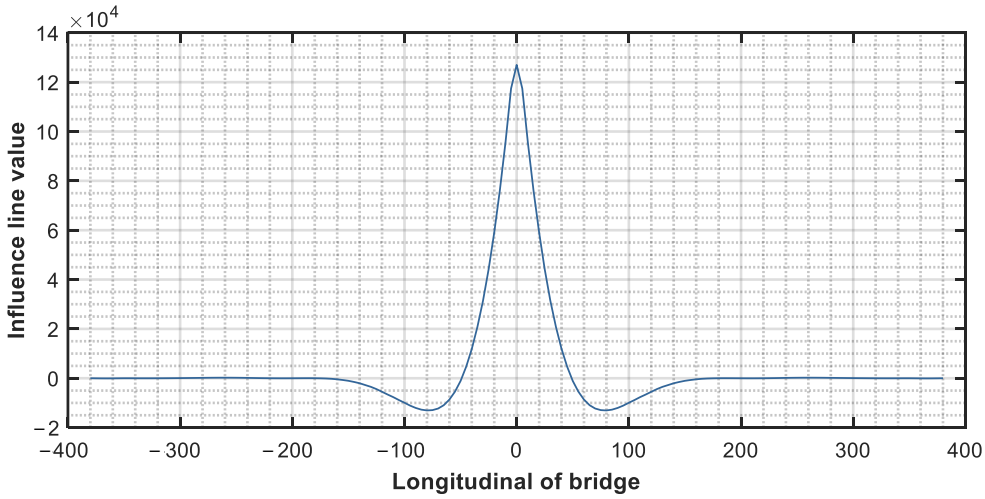

Figure 9. Diagram of virtual stress influence line of bridge.

Table 1. The traffic volume growth models.

Models	Equations
Model 1	$Veh^* = (year/a)^{1/b}$, a = 1434.25 and b = 0.031
Model 2	Veh = 60000/{1 + exp[−(a + b·$year$)]}, a = −95.87 and b = 0.05

Note: Veh^* is the annual average daily traffic.

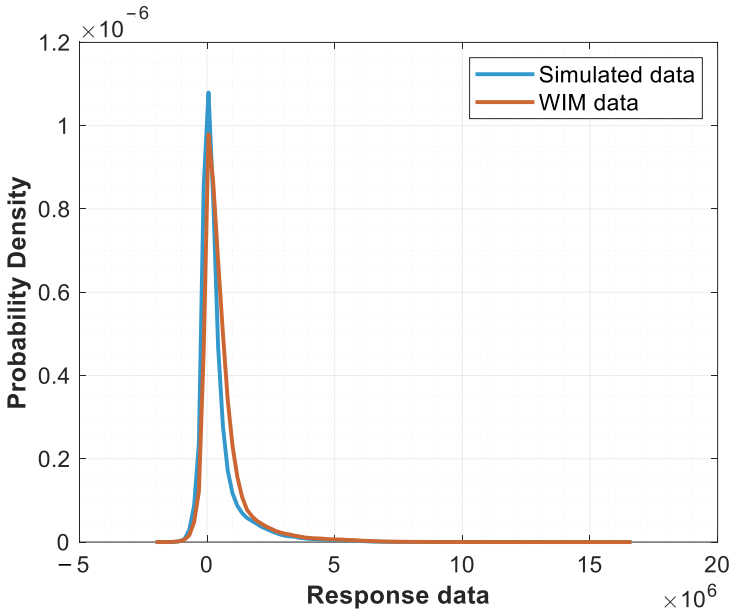

Figure 10. Probability density comparison of simulated traffic scenarios and WIM data responses.

The K-L divergence calculated from Equation (11) shows that the Kullback–Leibler divergence of the response data is 0.078232. This result indicates that the simulated data can characterize the WIM data distributions well.

6.2. Statistics of Variables

Probabilistic modeling of the variables is essential for carrying out the reliability evaluation. This study assumes that the critical fatigue damage index follows a lognormal distribution with a mean value of 1 and a standard deviation of 0.3, and the fatigue strength coefficient in terms of resistance is also assumed to follow a lognormal distribution with a mean value of 3.47×10^{14} and a standard deviation of 1.56×10^{14} [5]. The statistics of the variables in the LSF, including the equivalent stress range, S_{eq}, and the corresponding number of cycles, N_d, derived from both actual traffic flow data (i.e., WIM data) and the proposed traffic load model, are provided in Table 2.

Table 2. Probability distribution properties for fatigue analysis.

Variables	Mean Value	Standard Deviation	Distribution Type	Source
D_f	1.0	0.3	Lognormal	[51]
K_D	3.47×10^{14}	1.56×10^{14}	Lognormal	[51]
S_{eq}	10.2640	0.2709	Lognormal	
S^*_{eq}	9.6519	0.9049	Lognormal	
N_d	15,370.2	128.98	Lognormal	
N^*_d	16,614.0	1163.60	Lognormal	

Note: S^*_{eq} and N^*_d are calculated using the original WIM data loading.

6.3. Results and Discussion

The Monte Carlo method was applied to analyze fatigue reliability under different traffic flow conditions. The main computation involved is the simulation of traffic flow and the generation of fatigue stress histories based on pre-defined traffic parameters, which can be carried out relatively quickly using Monte Carlo simulations. The model does not require intensive training phases or complex optimization processes, which are characteristic of machine learning approaches like CA and Temporal Fusion Transformers [54]. A target fatigue reliability index of 2 was selected for this study, based on recommendations found in the literature [36,55], corresponding to a failure probability of 2.3%. Figure 11 shows the fatigue reliability under simulated traffic scenarios and WIM data without considering the continuous increase in traffic volume (i.e., the AADT is constant). Both the simulated and WIM data show a general decline in the reliability index over time. This decline reflects the progressive fatigue deterioration expected in structures under traffic load cycles. Through the refined simulated traffic flow method proposed in this study, it was found that the 162-year fatigue reliability index of the bridge is below 2. Based on the WIM data, the service time is 150 years. The reliability indices for the simulated data and the WIM data in the 100th year were reduced to 2.90 and 2.60, respectively. The intersection of the two lines in Figure 11 may be attributed to the high standard deviation of the WIM data. This is due to the inclusion of different traffic types, such as weekday and weekend variations. This difference shows the need for further optimization of the proposed model by simulating a broader range of traffic scenarios to capture mixed traffic flows more accurately.

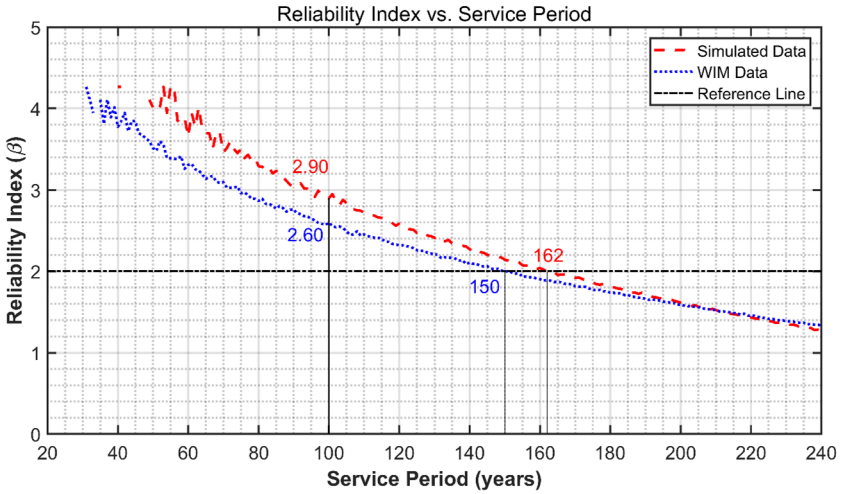

Figure 11. Fatigue reliability under simulated traffic scenarios and WIM data.

Figures 12 and 13 illustrate the results of fatigue reliability considering the traffic volume growth by using model 1 and model 2, respectively. The power regression law (model 1), representing continuous traffic demand growth, contrasts with the logistic distribution (model 2), which models a saturation point in vehicle numbers, simulating a cap on daily traffic flow at three times the bridge's original design load. The power regression model is ideal for scenarios where traffic growth is continuous, but it may overestimate long-term deterioration rates if traffic saturates. Conversely, the logistic regression model reflects saturation effects, providing more realistic predictions in capacity-constrained networks. Model 1 is suitable for urban bridges experiencing consistent growth due to high urbanization rates or critical economic corridors with continuous increases in freight traffic. Model 2 is particularly useful for bridges in areas with mature traffic infrastructure or where traffic growth is expected to stabilize due to economic or geographic constraints.

Under model 1, the service times for a fatigue reliability index below 2 were found to be 77 years (WIM data) and 80 years (simulated data). For the fatigue damage induced

by simulated traffic flow incorporating traffic growth, the point at which the fatigue reliability index reaches 2 is 82 years earlier than that without considering the traffic growth. Accounting for traffic growth using model 1 results in higher traffic demand prediction, which in turn leads to a more conservative estimation of the bridge's fatigue reliability. Consequently, the reliability index decreases more rapidly, reflecting an intensified risk due to the unbounded increase in traffic load effects. This implies that under the power regression model, the bridge may require earlier and more frequent maintenance interventions to mitigate the fatigue damage caused by increasing traffic loads.

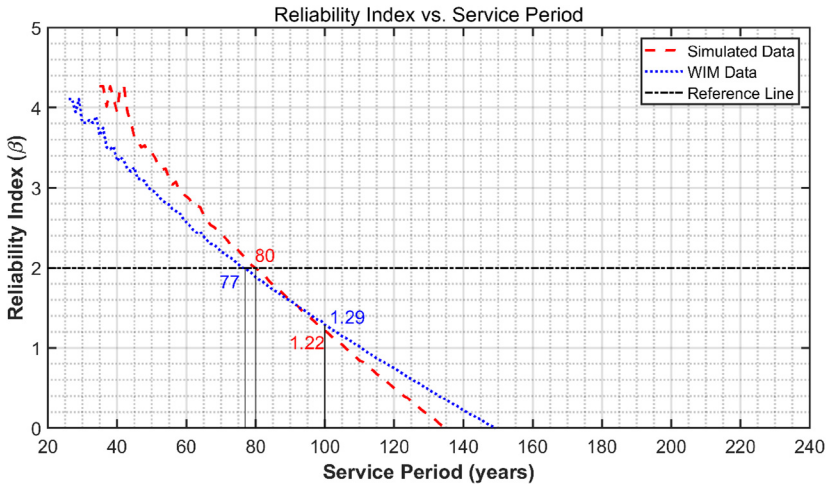

Figure 12. Fatigue reliability under traffic volume growth: model 1.

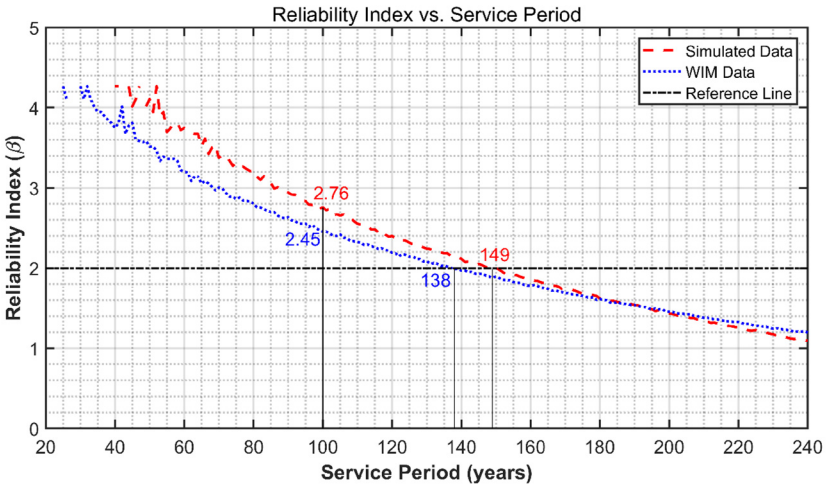

Figure 13. Fatigue reliability under traffic volume growth: model 2.

Model 2, utilizing a logistic regression approach, introduces a saturation point for traffic growth. Model 2 yields a more stable prediction of traffic demand, reflecting a plateau effect as traffic approaches the bridge traffic capacity limit. Accordingly, the reliability index decreases at a slower rate. Over a 100-year service life, the reliability indices calculated using both simulated data and WIM data decrease to 2.76 and 2.45, respectively. These results are close to those obtained without accounting for traffic growth and are significantly higher than those produced by model 1 (i.e., 1.22 for simulated data and 1.29 for WIM data). Using model 2 implies that the bridge fatigue reliability is preserved for a longer period under capped traffic growth conditions. The results suggest that different considerations of traffic load variations induced by traffic growth will result in significant differences in the bridge's fatigue evaluation results.

A comparison of these two models' results highlights the critical impact of the selected traffic growth assumptions on fatigue reliability assessments. The power model, while conservative, may overestimate the long-term deterioration rates if actual traffic growth reaches saturation. On the other hand, the logistic model could provide a more realistic assessment for infrastructure planning under anticipated traffic limits, balancing maintenance needs with expected traffic load scenarios. Furthermore, incorporating WIM data can enhance the models by providing empirical data, which can improve the accuracy of traffic load prediction, leading to more informed decisions regarding bridge maintenance and lifecycle management.

7. Conclusions

Traffic data measured by the WIM system offer a good basis for deriving traffic load models for the fatigue reliability assessment of road bridges. This study demonstrates a probabilistic approach for conducting fatigue reliability analyses of bridges under the influence of heavy traffic loads. By employing a Gaussian mixture model and a Poisson process, the probabilistic traffic model effectively captures the distribution and occurrence probability of heavy trucks based on real-world traffic data obtained from WIM technologies. The integration of the Nataf transformation method enables the consideration of correlations between key traffic load parameters, enhancing the model's accuracy. The proposed method provides a comprehensive framework for predicting bridge fatigue damage, offering significant improvements in the reliability and precision of fatigue life assessments for bridge structures under heavy traffic conditions.

Since traffic loading is a primary source of bridge fatigue, changes in traffic volume over the bridge's entire service life must be considered for accurate fatigue life prediction. Neglecting traffic growth could lead to an overly optimistic assessment of long-term structural reliability. Using the refined simulated traffic flow method proposed in this paper, it was found that the 80-year fatigue reliability index of the bridge falls below 2 when accounting for traffic flow growth modeled with a power regression law. Different traffic load growth models will result in significant differences in the bridge fatigue evaluation results. Appropriate consideration of traffic growth in fatigue reliability assessment is crucial for effective lifecycle management, as it allows for more accurate scheduling of maintenance interventions to ensure structural safety across the service life of bridges. The results of this case study are expected to support more informed decision-making in bridge maintenance and management strategies.

Future research will investigate the effects of different levels of GVW correlation and heavy truck platooning on bridge fatigue life. A comprehensive sensitivity analysis to identify the key parameters that most significantly affect the fatigue reliability of bridge components should be conducted. Additionally, the correlation between GVWs for traffic modeling should be determined using site-specific traffic data with appropriate statistical tools, ensuring the model's accuracy and applicability to real-world scenarios. These aspects will be explored in subsequent studies to provide a more robust understanding of traffic load effects on bridge reliability. Meanwhile, numerous fatigue life prediction methods have been proposed and applied over the years. Among these, data-driven approaches are particularly significant for assessing the service performance of steel bridges [56]. A comprehensive comparison should be conducted using state-of-the-art fatigue models and advanced deep learning techniques, such as the spatiotemporal embedding fusion transformer [54]. This model leverages attention mechanisms and feature fusion to effectively capture dynamic dependencies in traffic data. These investigations will lead to more precise models and predictive tools, advancing the reliability of bridge infrastructure in the face of traffic evolution.

Author Contributions: Conceptualization, M.Z. and X.W.; methodology, M.Z. and X.W.; validation, X.W. and Y.L.; writing—original draft preparation, M.Z.; writing—review and editing, X.W. and Y.L.; visualization, X.W.; supervision, Y.L.; project administration, M.Z.; funding acquisition, M.Z. All authors have read and agreed to the published version of the manuscript.

Funding: This research was funded by the National Natural Science Foundation of China, grant number 52208197.

Data Availability Statement: Data will be made available on request.

Conflicts of Interest: The authors declare no conflicts of interest.

References

1. Frøseth, G.T.; Rönnquist, A. Load model of historic traffic for fatigue life estimation of Norwegian railway bridges. *Eng. Struct.* **2019**, *200*, 109626. [CrossRef]
2. Jiang, C.; Wu, C.; Cai, C.S.; Xiong, W. Fatigue analysis of stay cables on the long-span bridges under combined action of traffic and wind. *Eng. Struct.* **2020**, *207*, 110212. [CrossRef]
3. Qin, S.; Zhang, J.; Huang, C.; Gao, L.; Bao, Y. Fatigue performance evaluation of steel-UHPC composite orthotropic deck in a long-span cable-stayed bridge under in-service traffic. *Eng. Struct.* **2022**, *254*, 113875. [CrossRef]
4. Wang, Y.; Fu, Z.; Ge, H.; Ji, B.; Hayakawa, N. Cracking reasons and features of fatigue details in the diaphragm of curved steel box girder. *Eng. Struct.* **2019**, *201*, 109767. [CrossRef]
5. Yang, D.; Guan, Z.; Yi, T.; Li, H.; Ni, Y. Fatigue Evaluation of Bridges Based on Strain Influence Line Loaded by Elaborate Stochastic Traffic Flow. *J. Bridge Eng.* **2022**, *27*, 04017086. [CrossRef]
6. ASCE. *Report Card for America's Infrastructure*; ASCE: Reston, VA, USA, 2013.
7. Farreras-Alcover, I.; Chryssanthopoulos, M.K.; Andersen, J.E. Data-based models for fatigue reliability of orthotropic steel bridge decks based on temperature, traffic and strain monitoring. *Int. J. Fatigue* **2017**, *95*, 104–119. [CrossRef]
8. British Standards Institution. *BS 5400-2: Steel, Concrete and Composite Bridges—Part 2: Specification for Loads*; BSI: London, UK, 2006.
9. AASHTO. *Highway Bridge Design Specifications*, 3rd ed.; AASHTO: Washington, DC, USA, 2004.
10. European Committee for Standardization. *Eurocode 1 Part 2: Traffic Loads on Bridges*; European Committee for Standardization: Brussels, Belgium, 2003.
11. *JTG D64-2015*; Specification for Design of Highway Steel Bridges. Ministry of Transport of the People's Republic of China; China Communications Press: Beijing, China, 2015.
12. U.S. Department of Transportation. *Beyond Traffic: 2045 Final Report*; Office of the Secretary of Transportation: Washington, DC, USA, 2016.
13. Leahy, C.; O'Brien, E.; O'Connor, A. The effect of traffic growth on characteristic bridge load effects. *Transp. Res. Procedia* **2016**, *14*, 3990–3999. [CrossRef]
14. Lu, N.; Beer, M.; Noori, M.; Liu, Y. Lifetime deflections of long-span bridges under dynamic and growing traffic loads. *J. Bridge Eng.* **2017**, *22*, 04017086. [CrossRef]
15. Han, W.S.; Wu, J.; Cai, C.S.; Chen, S.R. Characteristics and dynamic impact of overloaded extra heavy trucks on typical highway bridges. *J. Bridge Eng.* **2015**, *20*, 05014011. [CrossRef]
16. Ruan, X.; Zhou, J.; Shi, X.; Caprani, C.C. A site-specific traffic load model for long-span multi-pylon cable-stayed bridges. *Struct. Infrastruct. Eng.* **2017**, *13*, 494–504. [CrossRef]
17. Yuan, Y.; Han, W.; Huang, P.; Zhao, J.; Li, Y.; Zhang, J. Structure safety assessment under heavy traffic based on weigh-in-motion and simulation analysis. *Adv. Struct. Eng.* **2017**, *20*, 1864–1878. [CrossRef]
18. Ji, B.; Chen, D.; Ma, L.; Jiang, Z.; Shi, G.; Lv, L.; Xu, H.; Zhang, X. Research on stress spectrum of steel decks in suspension bridge considering measured traffic flow. *J. Perform. Constr. Facil.* **2011**, *26*, 65–75. [CrossRef]
19. Xu, D.; Xu, X.; Forde, M.C.; Caballero, A. Concrete and steel bridge Structural Health Monitoring—Insight into choices for machine learning applications. *Constr. Build. Mater.* **2023**, *402*, 132596. [CrossRef]
20. Li, X.; Kurata, M. Probabilistic Updating of Fishbone Model for Assessing Seismic Damage to Beam–Column Connections in Steel Moment-Resisting Frames. *Comput. Aided Civ. Inf. Eng.* **2019**, *34*, 790–805. [CrossRef]
21. Frangopol, D.M.; Strauss, A.; Kim, S. Bridge reliability assessment based on monitoring. *J. Bridge Eng.* **2008**, *13*, 258–270. [CrossRef]
22. Kwon, K.; Frangopol, D.M. Bridge fatigue reliability assessment using probability density functions of equivalent stress range based on field monitoring data. *Int. J. Fatigue* **2010**, *32*, 1221–1232. [CrossRef]
23. Ni, Y.Q.; Ye, X.W.; Ko, J.M. Monitoring-based fatigue reliability assessment of steel bridges: Analytical model and application. *J. Struct. Eng.* **2010**, *136*, 1563–1573. [CrossRef]
24. Di, J.; Ruan, X.; Zhou, X.; Wang, J.; Peng, X. Fatigue assessment of orthotropic steel bridge decks based on strain monitoring data. *Eng. Struct.* **2021**, *228*, 111437. [CrossRef]
25. Anitori, G.; Casas, J.R.; Ghosn, M. WIM-based live-load model for advanced analysis of simply supported short-and medium-span highway bridges. *J. Bridge Eng.* **2017**, *22*, 4017062. [CrossRef]
26. Anitori, G.; Casas, J.R.; Ghosn, M. Methodology for development of live load models for refined analysis of short and medium-span highway bridges. *Struct. Infrastruct. Eng.* **2018**, *14*, 477–490. [CrossRef]
27. Li, J.A.; Feng, D. Fatigue life evaluation of bridge stay cables subject to monitoring traffic and considering road roughness. *Eng. Struct.* **2023**, *293*, 116572. [CrossRef]

28. Kim, J.; Song, J. Bayesian updating methodology for probabilistic model of bridge traffic loads using in-service data of traffic environment. *Struct. Infrastruct. Eng.* **2023**, *19*, 77–92. [CrossRef]
29. Guo, T.; Frangopol, D.M.; Chen, Y. Fatigue reliability assessment of steel bridge details integrating weigh-in-motion data and probabilistic finite element analysis. *Comput. Struct.* **2012**, *112–113*, 245–257. [CrossRef]
30. Wang, X.; Ruan, X.; Casas, J.R.; Zhang, M. Probabilistic modeling of congested traffic scenarios on long-span bridges. *Appl. Sci.* **2024**, *14*, 9525. [CrossRef]
31. Wang, X.; Ruan, X.; Casas, J.R.; Zhang, M. Probabilistic model of traffic scenarios for extreme load effects in long-span bridges. *Struct. Saf.* **2024**, *106*, 102382. [CrossRef]
32. Wang, X.; Ruan, X.; Casas, J.R.; Zhang, M. Influence of the correlation of GVWs in the simulation of vehicle spatial distribution of extreme effects in long-span bridges. In *Bridge Maintenance, Safety, Management, Life-Cycle Sustainability and Innovations*; Taylor & Francis: London, UK, 2024; pp. 1255–1262.
33. Wang, F.Y.; Xu, Y.L. Traffic load simulation for long-span suspension bridges. *J. Bridge Eng.* **2019**, *24*, 05019005. [CrossRef]
34. Gao, R.; He, J.; Nie, Z. Stochastic Harmonic Function-Based Traffic Load Simulation Method for Fatigue Damage Assessment of Concrete Bridges. *Probabilistic Eng. Mech.* **2022**, *69*, 103308. [CrossRef]
35. Fan, Z.; Xu, X.; Ren, Y.; Chang, W.; Deng, C.; Huang, Q. Fatigue reliability analysis for suspenders of a long-span suspension bridge considering random traffic load and corrosion. *Structures* **2023**, *56*, 104981. [CrossRef]
36. Zhu, J.; Chen, Y.; Heng, J.; Wu, M.; Zhang, Y.; Li, Y. Probabilistic Corrosion-Fatigue Prognosis of Rib-to-Deck Welded Joints in Coastal Weathering Steel Bridges Exposed to Heavy Traffics. *Int. J. Fatigue* **2024**, *182*, 108210. [CrossRef]
37. Peng, X.; Wang, K.; Yang, Q.; Xu, B.; Di, J. Fatigue load model of orthotropic steel deck for port highway in China. *Front. Mater.* **2023**, *10*, 1115632. [CrossRef]
38. Ruan, X.; Zhou, J.; Tu, H.; Jin, Z.; Shi, X. An improved cellular automaton with axis information for microscopic traffic simulation. *Transp. Res. Part C Emerg. Technol.* **2017**, *78*, 63–77. [CrossRef]
39. O'Brien, E.J.; Lipari, A.; Caprani, C.C. Micro-simulation of single-lane traffic to identify critical loading conditions for long-span bridges. *Eng. Struct.* **2015**, *94*, 137–148. [CrossRef]
40. Chen, S.R.; Wu, J. Modeling stochastic live load for long-span bridge based on microscopic traffic flow simulation. *Comput. Struct.* **2011**, *89*, 813–824. [CrossRef]
41. Iervolino, I.; Baltzopoulos, G.; Vitale, A.; Grella, A.; Bonini, G.; Iannaccone, A. Empirical distributions of traffic loads from one year of weigh-in-motion data. *Sci. Data* **2023**, *10*, 289. [CrossRef]
42. Maljaars, J. Evaluation of traffic load models for fatigue verification of European road bridges. *Eng. Struct.* **2020**, *225*, 111326. [CrossRef]
43. Jin, S.; Qu, X.; Wang, D. Assessment of expressway traffic safety using Gaussian mixture model based on time to collision. *Int. J. Comput. Intell. Syst.* **2011**, *4*, 1122–1130.
44. Liu, X.; Han, W.; Yuan, Y.; Chen, X.; Xie, Q. Corrosion fatigue assessment and reliability analysis of short suspender of suspension bridge depending on refined traffic and wind load condition. *Eng. Struct.* **2021**, *234*, 111950. [CrossRef]
45. Nowak, A.S. Live load model for highway bridges. *Struct. Saf.* **1993**, *13*, 53–66. [CrossRef]
46. Nowak, A.S. Calibration of LRFD bridge design code. *J. Struct. Eng.* **1995**, *121*, 1245–1251. [CrossRef]
47. O'Brien, E.J.; Enright, B. Modeling same-direction two-lane traffic for bridge loading. *Struct. Saf.* **2011**, *33*, 296–304. [CrossRef]
48. Zhou, J.; Shi, X.; Caprani, C.C.; Ruan, X. Multi-lane factor for bridge traffic load from extreme events of coincident lane load effects. *Struct. Saf.* **2018**, *72*, 17–29. [CrossRef]
49. Nataf, A. Détermination des distributions de probabilité dont les marges sont donnée. *Comptes Rendus I'Académie Sci.* **1962**, *225*, 42–43.
50. *EN 1993-1-9*; Eurocode 3: Design of Steel Structures—Part 1–9: Fatigue. CEN (European Committee for Standardization): Brussels, Belgium, 2005.
51. The MathWorks Inc. *MATLAB*, version: 23.2.0 (R2023b); The MathWorks Inc.: Natick, MA, USA, 2023.
52. Pugliese, F.; De Risi, R.; Di Sarno, L. Reliability assessment of existing RC bridges with spatially-variable pitting corrosion subjected to increasing traffic demand. *Reliab. Eng. Syst. Saf.* **2022**, *218*, 108137. [CrossRef]
53. Bishop, C.M. *Pattern Recognition and Machine Learning*; Springer: Singapore, 2006.
54. Yang, H.; Wei, S.; Wang, Y. STFEformer: Spatial–Temporal Fusion Embedding Transformer for Traffic Flow Prediction. *Appl. Sci.* **2024**, *14*, 4325. [CrossRef]
55. Han, Y.; Li, K.; Cai, C.S.; Wang, L.; Xu, G. Fatigue reliability assessment of long-span steel-truss suspension bridges under the combined action of random traffic and wind loads. *J. Bridge Eng.* **2020**, *25*, 04020003. [CrossRef]
56. Feng, C.; Xu, L.; Zhao, L.; Han, Y.; Hao, K. A State-of-Art Review on Prediction Model for Fatigue Performance of Welded Joints via Data-Driven Method. *Adv. Eng. Mater.* **2023**, *25*, 2201430. [CrossRef]